

Integrative Aspects of Ventral Brainstem Function

The Intermediate Area and the Ventral Medulla

EUGENE E. NATTIE

Dartmouth Medical School
Lebanon, New Hampshire

I. Introduction

Part I of this book includes a number of presentations that describe the physiological roles of neurons located within the ventral aspect of the medulla oblongata. Many of these neurons have access from the surface of the ventrolateral medulla (VLM) and a surprising number of physiological systems appear to require input from these neurons for maintenance or modulation of their normal function. For the most part, experimental studies in each system (e.g., respiration, blood pressure regulation) have been performed in isolation without regard for other physiological systems. The outline below, which includes many of the papers of Part I, shows in brief the diversity of function represented within small regions of the ventral medulla and points out evidence indicating the importance of the ventral medullary neurons in these functions. The final (and speculative) section of the chapter asks why so many vital functions involve neurons with easy access to the VLM surface and what the functional significance of these neurons is.

II. The Intermediate Area

Cooling of the ventral medullary surface using temperatures that block function of neurons but not of passing axons can result in apnea and in decreased blood pressure (1-3). The most sensitive surface location for the respiratory effects, the intermediate area (IMA), lies adjacent to a similar area associated with potent blood pressure effects (see Ref. 4, this volume, for further discussion). Additional studies using surface application of neuroactive substances further described potent effects of a variety of these agents on breathing and blood pressure (see Refs. 4-6).

The specific neuroanatomical locus within the medulla of these effects due to perturbations of the VLM surface has been controversial. The blood supply to the brainstem arises at the ventral surface from penetrating arteries, which, together with their accompanying perivascular spaces, can allow rather deep penetration within the medulla of surface perturbations. This has been shown by evaluation of the rate and depth of penetration of small radiolabeled and larger molecules applied to the VLM surface (see Ref. 4, this volume, for discussion).

III. Possible Neuronal Substrates of the IMA

Some possible anatomical structures affected by these IMA surface experiments include the retrotrapezoid nucleus, the retrofacial nucleus, the subretrofacial region (including the C1 group), the *nucleus paragigantocellularis lateralis* (PGCL), midline and parapyramidal raphe neurons, the lateral reticular nucleus, and perhaps aspects of the rostral portion of the ventral respiratory group including the Bötzing and pre-Bötzing regions (see Ref. 4, this volume, for discussion). Here I will give a brief overview of some of these specific structures as they relate to this chapter.

The *retrotrapezoid nucleus* was identified by injection of retrograde anatomical tracers into major groups of respiratory neurons, which are located more dorsally. Labeling of a novel site lying ventral and ventromedial to the facial nucleus (within a few hundred micrometers of the VLM surface) led to this new anatomical definition (7). The retrotrapezoid nucleus was then found to contain neurons with respiratory-modulated as well as tonic firing patterns, both types increasing their firing rate with hypercapnia (see Ref. 4). Destruction of the retrotrapezoid nucleus region unilaterally can result in depression of respiratory output (including apnea) and absent chemosensitivity, suggesting an important role for these respiratory neurons (see Ref. 4). Such lesions have little effect on blood pressure.

Bilateral (8) and unilateral (9) electrolytic and chemical lesions within the *retrofacial nucleus* of the cat can also result in decreased respiratory output and

chemosensitivity. The retrofacial and subretrofacial regions have neurons with respiratory-modulating firing patterns, some of which have processes that extend to the surface of the VLM (10,11). The retrofacial region has known respiratory involvement, while the subretrofacial region is important in blood pressure regulation (see below). At quite discrete sites located more caudally and deeper, bilateral injections of glutamate receptor antagonists can also produce apnea in anesthetized animals (12,13).

The PGCL (14,15) lies between the VLM surface and the nucleus ambiguus. It extends rostrally from the lateral reticular nucleus to the region medial to the facial nucleus lying just lateral to the inferior olive. It is essentially just beneath the center of the IMA. Retrograde tracing experiments have shown that afferent inputs converge there from a variety of sites, including the spinal cord, caudal lateral medulla, contralateral PGCL, nucleus of the solitary tract, A1 area, lateral parabrachial nucleus, Kölliker-Fuse nucleus, periaqueductal gray, and supraoculomotor nucleus (14). Studies of retrograde transport from injections limited to the juxtafacial portion of PGCL (15) show a different but also diverse pattern of afferent sources, including the dorsal column nuclei, inferior colliculus, paralemniscus, paramedian reticular formation, paraolivary reticular formation, retrofacial PGCL, caudal medullary reticular formation, and dorsal periaqueductal gray. The PGCL seems to be a source of convergence of many afferent inputs involved in pain, analgesia, cardiovascular control, respiratory control, exteroceptive sensation, and arousal. A major source of efferents from the PGCL is the locus ceruleus, which itself has widespread inputs to the higher nervous system and is thought to be primarily involved in arousal and vigilance (16).

Parapyramidal neurons of the midline raphe lie at sites accessible to surface applications at the IMA (17). While the raphe has been studied largely in regard to cardiovascular control (see Ref. 18, for example), there is evidence that this region is involved in respiratory control as well (19,20). Parapyramidal cells have also been implicated in the control of breathing by localized surface cooling experiments (21).

Thus, there are a number of defined anatomical structures, accessible to substances applied to the surface of the VLM, which are likely sites of physiological effects on respiratory and blood pressure regulation. The nomenclature used for these structures has evolved more from an anatomical than a functional rationale. From the studies cited above (and in Ref. 4), it appears that a rostral-to-caudal column of neurons exists in the VLM with involvement in the control of respiration and blood pressure (and in other functions discussed below). Cardiorespiratory neurons in the column appear to be distributed among a number of these (and other) anatomically designated structures. Much more detailed examination of the lateral tegmental field has led to a similar conclusion: that respiratory control neurons of the ventral respiratory group are distributed among a number of discrete anatomical nuclei (22,23).

IV. Central Chemoreceptors; CO₂

The traditional view of central chemoreception has focused on the VLM as the chemoreceptor locus, based largely on studies that used alterations in surface pH as the localizing stimulus. Some workers have criticized this interpretation and much of the evidence for and against this idea is reviewed in Ref. 4.

In my laboratory, we have used microinjections of 1 nL acetazolamide to produce focal regions of reversible tissue acidosis (see Refs. 4 and 24 for details). The results indicate that central chemoreception is located at widespread sites within the brainstem, including (1) the nucleus tractus solitarius, (2) the vicinity of the locus ceruleus, and (3) within 800 μm of the VLM surface at sites probably accessible from the VLM surface, as originally proposed. Ongoing work suggests the involvement of other sites as well (25).

Of interest in the role of the VLM in chemoreception are the measurements of tissue pH profiles during hypercapnia induced by injection of hypercapnic saline into the vertebral artery (26). Surprisingly, at some sites the pH decreased significantly and at others it did not change. The sites with large pH changes, proposed as the location of central chemoreceptors, were located in the vicinity of the nucleus tractus solitarius, within the nucleus ambiguus, and, again, near the VLM surface as originally proposed.

In this volume, data was presented from brainstem staining for the c-fos gene product following application of acidic pledgets to the caudal VLM surface (Ref. 27, this volume). The stained regions were surprising in their number and distribution throughout the caudal to rostral axis of the brainstem. While it is difficult to evaluate the specificity of such c-fos experiments, the widespread nature of neuronal stimulation from such a localized surface application emphasizes the number of connections of neurons accessible from the VLM surface. An alternative approach, optical imaging following systemic changes in CO₂, O₂, and blood pressure, indicated a rather widespread involvement of VLM neurons with altered function (Ref. 28, this volume). This approach has value in discerning patterns of involvement of neurons within a finite distance of the VLM surface and suggests discrete patterns of neuron involvement that are specific for the different stimuli.

In respect to the VLM, central chemoreception exists within a few hundred micrometers of the VLM surface at sites from the level of the hypoglossal nerve rootlets rostrally to the level of the trapezoid body. Stimulation by CO₂ or H⁺ at these sites can stimulate respiratory output and large numbers of medullary neurons. A small number of observations from my lab suggests that some central chemoreceptor sites may be specific for blood pressure regulation, others for respiration (24).

V. Central Chemoreception; O₂

While the primary transduction of a hypoxic stimulus that increases respiration occurs at the carotid body, there are some interesting effects of hypoxia

which are localized to the VLM. In the ventilatory acclimatization to chronic hypoxia, the role of central chemoreceptors and the VLM has been controversial. One hypothesis described the prolonged increase in ventilation seen with acclimatization to acidic changes in cerebral fluids (29). It seems clear that large-cavity cerebrospinal fluid pH is not acidic under these conditions (30). But VLM tissue pH in some regions does become acidic under hypoxic conditions (30). For example, in anesthetized cats, 5 min of isocapnic hypoxia such as to decrease arterial oxygen saturation to 48% results in regional VLM acidosis. The pH was decreased at rostral and caudal VLM regions but not at the IMA (31). This is reminiscent of the regional VLM pH changes observed following vertebral artery injection of hypercapnic saline (see above). It is possible that such changes participate in the increase in respiration observed in acclimatization. Respiration in adult animals is not stimulated by hypoxia (and the presumed VLM regional acidosis) following denervation of the peripheral chemoreceptors. But it seems reasonable to hypothesize that central chemoreceptor stimulation by local hypoxia-induced acidosis may potentiate the hypoxic ventilatory response in animals with intact peripheral chemoreceptors. The suggestion that the response to acute peripheral chemoreceptor stimulation involves an input from neurons in the VLM region (see Ref. 32, this volume, for discussion) adds support to this hypothesis.

There is evidence suggesting a possible role for VLM neurons in sensing changes in metabolism, perhaps via tissue hypoxia. First, the stimulation of respiration produced by infusion of 2,4-dinitrophenol can be blocked by cooling or destruction of the VLM at the IMA (33). Second, immunohistochemistry has localized the enzyme involved in nitric oxide metabolism, NADPH diaphorase, in a 2-mm long column of cells lying lateral to the inferior olive and medial to the C1 cell group in the rostral VLM (RVLM) (34). Third, specifically identified RVLM neurons involved in blood pressure regulation have been described that can be stimulated by local injections of sodium cyanide and by the production of hypoxia (arterial PO₂ = 27 mm Hg) even following removal of peripheral chemoreceptor tissue (35). Nearby respiratory neurons were not excited by these stimuli. These neurons excited by hypoxia appear to be the source of the central ischemic pressor response.

VI. Airways

Neurons in the caudal VLM stimulated by activation of group III and IV hind-limb afferents are involved in the decrease in airway resistance observed in such conditions (see Ref. 36, this volume). Neurons in more rostral sites can be stimulated by muscle contraction and produce a pressor response (Ref. 36, this volume). The VLM neurotransmitters involved may include glutamate, as microinjections of glutamate receptor antagonists attenuate these bronchodilator and pressor responses (Ref. 36, this volume).

Other airway responses can be affected by VLM neurons. Application to the VLM surface at the IMA of agents that block or stimulate the function of accessible neurons can alter (1) CO₂-sensitive respiratory phasic changes in nasal patency, (2) hypoglossal nerve activity affecting upper airway patency, (3) the pharyngeal response to pulmonary irritant receptor stimulation, (4) the tone of tracheal smooth muscle, and (5) the secretion of tracheal glands (32).

VII. Breathing

The studies discussed above, which showed profound effects on respiratory output and chemosensitivity with surface cooling at the IMA and lesions of more specific anatomical sites beneath the IMA, were performed in anesthetized or decerebrate animals. Of great interest are the results of similar studies in conscious animals. Conscious cats following bilateral coagulation of the IMA have decreased respiration and CO₂ retention and decreased responsiveness to CO₂ (37,38). Cooling of the IMA in conscious goats also depresses ventilation at rest, in response to hypercapnia, and in exercise (Ref. 39 and H. V. Forster, personal communication). In conscious dogs, after unilateral lesioning of the retrotrapezoid region by kainic acid injections, periods of cluster breathing have been observed (40). In humans with neurological disease of the brainstem resulting in unilateral lesions of the RVLM, ventilation and CO₂ sensitivity are decreased and apneas during sleep are more common (41). And in victims of sudden infant death syndrome, some show abnormally few neurons in a region of the rostral ventrolateral medulla (42). Changes in airway caliber related to VLM neuronal function have not been evaluated in conscious animals.

Neurons located within a small region of the VLM just medial to the caudal aspect of the facial nucleus, close to the surface (43), and within a region just caudal to the level of the retrofacial nucleus—the pre-Bötzing region (44,45)—have been proposed to be the site of respiratory rhythm generation, at least in the neonatal rat brainstem preparation. This is a difficult preparation in that it has a hypoxic central core with a viable outside ring of tissue approximately 800 μm in thickness (46). Yet the similarity of the anatomical location of these proposed regions for respiratory rhythmogenesis and those in adult mammals where cooling or lesioning have dramatic effects on respiratory output is striking.

VIII. Blood Pressure

Surface manipulations at and near to the IMA often had blood pressure as well as respiratory effects. Subsequent studies identified a subretrofacial pressor region (47), also called the C1 region (48), which includes a large portion of the PGCL. Neurons of this pressor region project to the intermediolateral column

of the spinal cord, may contain catecholamines, and are thought important in the origin and maintenance of sympathetic tone to the cardiovascular system. Conditional pacemaker neurons, thought to be cardiovascular in function, have been reported here (49), and the link between respiratory and cardiovascular sympathetic output, whereby a large portion of cardiovascular sympathetic tone is phasically related to phrenic output, occurs here (50). The neurons in this rostral pressor region lie just caudal and dorsal to the retrotrapezoid nucleus, within the region ventral to the retrofacial nucleus. Within the RVLM, there appears to be a functional organization of the neurons into discrete groups that have specific vascular bed connections (51,52). This rostral pressor region can also be divided anatomically into three subregions: the midline raphe, PGCL, and rostroventrolateral reticular nucleus (53). This RVLM pressor region also has anatomical connections to the periaqueductal gray (18), the lateral parabrachial nucleus, the locus ceruleus, and the lateral hypothalamic area (54) and the amygdaloid complex (55). It receives widespread afferents (see Ref. 56, for example) and it can modulate cardiovascular reflexes at the nucleus tractus solitarius (57). Bilateral lesions of the C1 region can result in decreased blood pressure (to spinal levels) and abolish pressor sympathetic outflow (48,58).

Neurons responsive to serotonin receptor agonists (producing a hypotensive effect) lie in the midline raphe and at the parapyramidal region of the RVLM (59). And a more caudal region of the VLM appears to be involved in depressor responses (60,61). A single study suggests involvement of neurons in the midline raphe in the control of pulmonary blood flow. Injections of a glutamate agonist and toxin, ibotenic acid, into the raphe of the rat results in increased pulmonary artery pressure, hypoxemia, acidosis, hypothermia, and death without any evidence of pulmonary edema (62).

IX. Nociception

Neurons in the rostral ventromedial medulla are part of a network involved with control of pain transmission. They are located in the nucleus raphe magnus, the nucleus PGCL, and the adjacent reticular network, and they have been characterized by their projections to spinal cord and their responses to painful stimuli and opiate analgesic agents. Noxious stimuli to the extremities result in withdrawal of the paw and either increased (on cells) or decreased (off cells) firing rates of these neurons (63). The off cells are excited by opiate analgesic agents, suggesting that they have an inhibitory effect on pain transmission (63). Of particular interest is the fact that increased CO₂ can increase the threshold for painful stimuli, possibly via an endogenous opiate-related mechanism (64). This effect could well be occurring at this region of the VLM, where nociceptive and respiratory neurons are in close proximity. Of similar interest is the observation that application of opiates onto the VLM surface at the rostral aspect of the IMA can result in respiratory depression (65). And the hypoten-

sive and respiratory depressant responses to cocaine application on the VLM surface at more caudal locations can be prevented in part by prior treatment at these sites with an anticholinesterase (see Ref. 66, this volume for discussion).

A specific role of PGCL neurons, which are easily accessible from the VLM surface, in the transmission of peripheral pain to the locus ceruleus has been demonstrated. Injections of lidocaine into the ventromedial PGCL attenuate the response of single neurons within the locus ceruleus to foot shock in the anesthetized rat (67).

X. Vestibular System

The stimulation of vestibular afferents has effects on autonomic and respiratory output (see Ref. 68, this volume). Neurons in the VLM rostral pressor region and the more caudal depressor region with known connections to the sympathetic preganglionic neurons respond with an increased firing rate to vestibular stimulation. There is a specificity to the VLM connections in that their input comes largely from otolith organs and they have a greater response to pitch than to roll.

XI. Why Are So Many Functions Attributed to Neurons So Close to Each Other and to the VLM Surface? What Is the Functional Significance of These Rostral VLM Neurons?

These are speculative questions without proven answers at present. In respect to the proximity to the VLM surface, one thought is that the projections to the surface of many neurons lying within the VLM allows them to sense or sample the cerebrospinal fluid (CSF) coming into contact with the surface as it flows by in its course through the ventricular system. There are substances in the CSF that might reflect activity at other more central sites within the neuroaxis or in blood via entry through regions having a less stringent blood-brain barrier (see Ref. 69, this volume, for example). These could be sensed at the VLM surface. This seems to me to be a rather unlikely possibility, given the incredibly diverse neuronal signaling possibilities in both the anatomical and synaptic realms. Also, the turnover for CSF is rather slow, giving this idea of sensing important stimuli via CSF a rather phlegmatic potential in respect to speed of response. Alternatively, if substances in CSF reflect some time average of central nervous system events or state, then this type of signaling system could be of value, allowing medullary autonomic neurons to monitor higher cerebral events in a slow, stately manner.

A second possibility to explain the location of these neurons near the VLM surface relates to the blood supply to the brainstem, which enters from the

ventral surface via penetrating arteries. Any investigator who has examined the ventral medullary surface under the operating microscope can vouch for the impressive number of blood vessels both on the surface and entering into the parenchyma. These could provide a means for nearby neurons within the VLM to sample what is happening in the blood. This possible explanation would have to include an evaluation of the significance of the blood-brain barrier, which is intact in this region.

Third, the location of all of these important physiological effects to neurons lying close together within the VLM may just be coincidence. The entire brainstem is very compact, and other brainstem regions—e.g., the nucleus tractus solitarius (NTS) (see Ref. 70, for example) and the lateral tegmental field (22, 23)—are known to have many functions expressed within a small anatomical region.

I argue here that compelling evidence supports the hypothesis that neurons within the VLM have a particularly important role in the control of respiration and blood pressure. In respiratory regulation, specific lesions of small VLM regions and cooling of larger surface areas (cited above) have dramatic effects on respiratory output and reflexes even in chronic conscious preparations. Similar or larger lesions in other medullary (71) and pontine (72) regions known to be involved in respiratory regulation do not have such effects. In blood pressure regulation, again, specific VLM lesions dramatically reduce cardiovascular sympathetic outflow, even in chronic conscious preparations (see Ref. 58). The most effective lesion location for the blood pressure effects is not the same as that for the respiratory effects, although they are in proximity. While lesion studies do have problems and recent reviews (70) have downplayed any special significance of the RVLM in blood pressure regulation, I find the hypothesis for a specific and significant role for these RVLM cardiorespiratory neurons to be of interest and worthy of continued investigation.

What are the physiological roles of these RVLM neurons that are important in respiratory and blood pressure regulation? Early work on the IMA emphasized the word *integration*—that the IMA is an integrative area (3,37). There is ample evidence that these neurons receive afferents from many central and peripheral sources (cited above). In fact, single neurons located near these RVLM sites have been shown to receive multiple afferent inputs, which converge on them (73). However, most cardiovascular and respiratory peripheral afferents have their primary synapse in the more dorsally located NTS. The functional relationship between the RVLM and the NTS is unclear. Recent evidence (cited above) has shown that RVLM neurons can modulate specific reflexes at the NTS. Thus, RVLM neurons may integrate afferent information, and they can modify reflexes at other medullary sites. This region of the VLM also contains CO₂/H⁺ chemoreceptor function, as shown by studies from my own lab using 1-nL injections of acetazolamide to produce focal acidosis (as well as other studies reviewed in Ref. 4), and it contains hypoxia-sensitive neurons (cited above).

I propose that, in addition to receiving afferent information, modifying reflexes at other sites, and containing chemosensitive elements, the cardiovascular and respiratory neurons of the rostral VLM provide a tonic input or drive to the neuronal networks involved in these respective control systems, an input that sustains these networks in an active state. This is not a new suggestion (74). And recent work in conscious goats with cooling of the rostral VLM surface shows decreased respiratory output in eucapnic, hypercapnic, hypoxic, and exercise conditions but no disruption of rhythm generation (Forster H. V., personal communication), observations supporting this hypothesis. Recent work from my lab has shown significant long-term stimulation of phrenic activity following single injections of glutamate (100 mM; 10 nL) into the RTN of the cat (75), again supporting this hypothesis. An analogy for this hypothesis in a better understood neural network is the driver or P cell for the pyloric rhythm of the crustacean stomatogastric ganglion (76). Specific destruction of these cells reduces the rhythmic output of this network into tonic activity. In mammals, there is evidence that afferent input is required for the respiratory control system to maintain a rhythmic output and that there is a tonic respiratory drive independent of the afferent determined rhythmic output (77,78). Is it possible that the source of this tonic drive is these rostral VLM neurons?

Acknowledgment

The author is supported by NIH RO1 HL28066.

References

1. Cherniack NS, von Euler C, Homma I, Kao FF. Graded changes in central chemoreceptor input by local temperature changes on the ventral surface of the medulla. *J Physiol (Lond)* 1979; 287:191-211.
2. Millhorn DE, Eldridge FL, Waldrop TG. Effects of medullary area $I_{(s)}$ cooling on respiratory response to chemoreceptor inputs. *Respir Physiol* 1982; 49:23-39.
3. Schläpke ME, See WR, Loeschcke HH. Ventilatory response to alterations of H^+ ion concentration in small areas of the ventral medullary surface. *Respir Physiol* 1970; 10:198-212.
4. Nattie EE, Li A, Coates EL. Central chemoreceptor location and the ventrolateral medulla (this volume).
5. Millhorn DE, Eldridge FL. Role of ventrolateral medulla in regulation of respiratory and cardiovascular systems. *J Appl Physiol* 1986; 61:1249-1263.
6. Bruce EN, Cherniack NS. Central chemoreceptors (brief review). *J Appl Physiol* 1987; 62:389-402.
7. Smith JC, Morrison DE, Ellenberger HH, et al. Brainstem projections to the major respiratory neuron populations in the medulla of the cat. *J Comp Neurol* 1989;281: 69-96.

8. St. John WM, Hwang Q, Nattie EE, Zhou D. Functions of the retrofacial neurons in chemosensitivity and ventilatory neurogenesis. *Respir Physiol* 1989; 76:159-172.
9. Nattie EE, Blanchford C, Li A. Retrofacial lesions: Effects on CO_2 sensitive phrenic and sympathetic activity. *J Appl Physiol* 1992; 73:1317-1325.
10. Bianchi AL, Grélot L, Iscoe S, Remmers JE. Electrophysiological properties of rostral medullary respiratory neurones in the cat: An intracellular study. *J Physiol (Lond)* 1988; 407:293-310.
11. Pilowsky PM, Jiang C, Lipski J. An intracellular study of respiratory neurons in the rostral ventrolateral medulla of the rat and their relationship to catecholamine-containing neurons. *J Comp Neurol* 1990; 301:604-617.
12. Abrahams TP, Hornby PJ, Walton DP, et al. An excitatory amino acid(s) in the ventrolateral medulla is (are) required for breathing to occur in the anesthetized cat. *J Exp Pharm Ther* 1991; 259:1388-1395.
13. Jung R, Bruce EN, Katona PG. Cardiorespiratory responses to glutaminergic antagonists in the caudal ventrolateral medulla of rats. *Brain Res* 1991; 564:286-295.
14. Van Bockstaele EJ, Pieribone VA, Aston-Jones G. Diverse afferents converge on the nucleus paragigantocellularis in the rat ventrolateral medulla: Retrograde and anterograde tracing studies. *J Comp Neurol* 1989; 290:561-584.
15. Van Bockstaele EJ, Akaoka H, Aston-Jones G. Brainstem afferents to the rostral (juxtafacial) nucleus paragigantocellularis: Integration of exteroceptive and interoceptive sensory inputs in the ventral tegmentum. *Brain Res* 1993; 603:1-18.
16. Aston-Jones G, Ennis VA, Pieribone VA, et al. The brain nucleus locus coeruleus: Restricted afferent control of a broad efferent network. *Science* 1986; 234:734-737.
17. Helke CJ, Thor KB, Sasek CA. Chemical neuroanatomy of the parapyramidal region of the ventral medulla in the rat. In: Ciriello J, Caverson MM, Polosa E, eds. *The Central Organization of Cardiovascular Control*. New York: Elsevier, 1989: 17-28.
18. Wang WH, Lovick TA. The inhibitory effect of the ventrolateral periaqueductal grey matter on neurones in the rostral ventrolateral medulla involves a relay in the medullary raphe nuclei. *Exp Brain Res* 1993; 94:295-300.
19. Holtman JR Jr, Anastasi NC, Norman WP, Dretchen KL. Effect of electrical stimulation of the raphe obscurus on phrenic nerve activity in the cat. *Brain Res* 1986; 362:214-220.
20. Holtman JR Jr, Marion LJ, Speck DF. Origin of serotonin-containing projections to the ventral respiratory group in the rat. *Neuroscience* 1990; 37:541-552.
21. Fukuda Y, Tojima H, Tanaka K, Chiba T. Respiratory suppression by focal cooling of ventral medullary surface in anesthetized rats: Functional and neuroanatomical correlate. *Neurosci Lett* 1993; 153:177-180.
22. Ellenberger HH, Feldman JL, Shan W-Z. Subnuclear organization of the lateral tegmental field. II: Catecholamine neurons and ventral respiratory group. *J Comp Neurol* 1990; 294:212-222.
23. Ellenberger HH, Feldman JL. Subnuclear organization of the lateral tegmental field. I: Nucleus ambiguus and ventral respiratory group. *J Comp Neurol* 1990; 294: 202-211.
24. Coates EL, Li A, Nattie EE. Widespread sites of brainstem ventilatory chemoreceptors. *J Appl Physiol* 1993; 75:5-14.
25. Bernard DG, Li A, Nattie EE. Ventilatory chemoreceptors in the midline brainstem raphe of rats. *Soc Neurosci Abst* 1994; 20:959.

26. Arita H, Ichikawa K, Kuwana S, Kogo N. Possible locations of pH-dependent central chemoreceptors: Intramedullary regions with acidic shift of extracellular fluid pH during hypercapnia. *Brain Res* 1989; 485:285-293.
27. Douglas RM, Trough CO, Melville GN, et al. Localization of c-FOS protein in rat brainstem in response to the topical application of acidic mock cerebrospinal fluid (this volume).
28. Gozal D, Rector DM, Harper RM. Functional assessment of the ventral medullary surface by optical imaging (this volume).
29. Fencl V, Gabel RA, Wolfe D. Composition of cerebral fluids in goats adapted to high altitude. *J Appl Physiol* 1979; 47:508-513.
30. Musch TI, Dempsey JA, Smith CA, et al. Metabolic acids and $[H^+]$ regulation in brain tissue during acclimatization to chronic hypoxia. *J Appl Physiol* 1983; 55:1486-1495.
31. Xu F, Sato M, Spellman MJ Jr, et al. Topography of cat medullary ventral surface hypoxic acidification. *J Appl Physiol* 1992; 73:2631-2637.
32. Haxhiu MA, Loewy AD, Cherniack NS. Ventral medullary network and airway control (this volume).
33. Prabhakar NR, Mitra J, Adams EM, Cherniack NS. Involvement of ventral medullary surface in respiratory responses induced by 2,4-dinitrophenol. *J Appl Physiol* 1989; 66:598-605.
34. Iadecola C, Faris PL, Hartman BK, Xu Y. Localization of NADPH diaphorase in neurons of the rostral ventral medulla: Possible role of nitric oxide in central autonomic regulation and oxygen chemoreception. *Brain Res* 1993; 603:173-179.
35. Sun MK, Reis DJ. Hypoxia selectively excites vasomotor neurons of rostral ventrolateral medulla in rats. *Am J Physiol (Regul Integrat Comp Physiol 35)* 1994; 266:R245-R256.
36. Solomon IC. Role of the caudal ventrolateral medulla in the reflex bronchodilation arising from the hindlimb (this volume).
37. Schläpke ME. Elimination of central chemosensitivity by coagulation of a bilateral area on the ventral medullary surface in awake cats. *Pflügers Arch* 1979; 379:231-241.
38. Burghardt F, Schläpke ME. Loss of central chemosensitivity: An animal model to overcome respiratory insufficiency. *J Auton Nerv Syst* 1986; (suppl):105-109.
39. Pan LG, Forster HV, Erickson BK, Lowry T. Effect of transient cooling of the ventral surface of the medulla (VLM) in awake goats. *FASEB J* 1991; 5:A665.
40. Dormer KJ, Bedford TG. Cardiovascular control by the rostral ventrolateral medulla in the conscious dog. In: Ciriello J, Caverson MM, Polosa E, eds. *The Central Neural Organization of Cardiovascular Control*, Progress Brain Research 81. Amsterdam: Elsevier, 1981:265-277.
41. Guz A. Brain-stem lesions in man with loss, or reduction of, ventilatory responses to CO_2 : Implications of breathing at rest and on exercise. *Intern Union Physiol Sci Abst* 1993; 32:25.
42. Filiano JJ, Choi JC, Kinney HC. Arcuate nucleus hypoplasia in the sudden infant death syndrome. *J Neuropathol Exp Neurol* 1992; 51:394-403.
43. Onimaru H, Arata A, Homma I. Localization of respiratory rhythm-generating neurons in the medulla of brainstem-spinal cord preparations from newborn rats. *Neurosci Lett* 1987; 78:151-155.

44. Smith JC, Ellenberger HH, Ballanyi K, et al. Pre-Bötzinger complex: A brainstem region that may generate respiratory rhythm in mammals. *Science* 1991; 254:726-729.
45. Smith JC, Ballanyi K, Richter DW. Whole-cell patch-clamp recording from respiratory neurons in mammalian brainstem in vitro. *Neurosci Lett* 1992; 134:153-156.
46. Brockhaus J, Ballanyi K, Smith JC, Richter DW. Microenvironment of respiratory neurons in the in vitro brainstem-spinal cord of neonatal rats. *J Physiol (Lond)* 1993; 462:421-445.
47. Dampney R. The subretrofacial nucleus: Its pivotal role in cardiovascular regulation. *News Physiol Sci* 1990; 5:63-66.
48. Reis DJ, Ross C, Granata AR, Ruggiero DA. Role of C1 area of rostromedullary lateral medulla in cardiovascular control. In: Buckley JP, Ferrario CM, eds. *Brain Peptides and Catecholamines in Cardiovascular Regulation*. New York: Raven Press, 1987:1-14.
49. Sun M-K, Young BS, Hackett JT, Guyenet PG. Reticulospinal pacemaker neurons of the rat rostral ventrolateral medulla with putative sympathoexcitatory function: an intracellular study "in vitro." *Brain Res* 1988; 442:229-239.
50. Guyenet P, Darnall RA, Riley TA. Rostral ventrolateral medulla and sympatho-respiratory integration in the rat. *Am J Physiol (Regul Integrat Comp Physiol 28)* 1990; 259:R1063-R1074.
51. Dean C, Seagard JL, Hopp FA, Kampine JP. Differential control of sympathetic activity to kidney and skeletal muscle by ventral medullary neurons. *J Auton Nerv Syst* 1992; 37:1-10.
52. McAllen RM, Dampney RAL. Vasomotor neurons in the rostral ventrolateral medulla are organized topographically with respect to type of vascular bed but not body region. *Neurosci Lett* 1990; 110:91-96.
53. Zagon A. Innervation of serotonergic medullary raphe neurons from cells of the rostral ventrolateral medulla. *Neuroscience* 1993; 55:849-867.
54. Agarwal SK, Calaresu FR. Supramedullary inputs to cardiovascular neurons of rostral ventrolateral medulla in rats. *Am J Physiol (Regul Integrat Comp Physiol)* 1993; 265:R111-R116.
55. Roder S, Ciriello J. Innervation of the amygdaloid complex by catecholaminergic cell groups of the ventrolateral medulla. *J Comp Neurol* 1993; 332:105-122.
56. Ermirio R, Ruggeri P, Molinari C, Weaver LC. Somatic and visceral inputs to neurons of the rostral ventrolateral medulla. *Am J Physiol (Regul Integrat Comp Physiol)* 1993; 265:R35-R40.
57. Roder S, Ciriello J. Convergence of ventrolateral medullary and aortic baroreceptor inputs in nucleus of the solitary tract. *Cand J Physiol Pharm* 1993; 71:365-373.
58. Cochrane KL, Nathan MA. Cardiovascular effects of lesions of the rostral ventrolateral medulla and the nucleus reticularis parvocellularis in rats. *J Auton Nerv Syst* 1993; 43:69-81.
59. Helke CJ, McDonald CH, Phillips ET. Hypotensive effects of 5-HT_{1A} receptor activation: Ventral medullary sites and mechanisms of action in the rat. *J Auton Nerv Syst* 1993; 42:177-188.
60. Cravo SL, Morrison SF. The caudal ventrolateral medulla is a source of tonic sympathoinhibition. *Brain Res* 1993; 621:133-136.

61. Willette RN, Barcas PP, Krieger AJ, Sapru HN. Vasopressor and depressor areas in the rat medulla: Identification by microinjection of L-glutamate. *Neuropharmacology* 1983; 22:1071-1079.
62. Carruth MK, Fowler AA, Fairman RP, et al. Respiratory failure without pulmonary edema following injection of a glutamate agonist into the ventral medulla of the rat. *Brain Res Bull* 1992; 28:365-378.
63. Fields HL, Barbaro NM, Heinricher MM. Brain stem neuronal circuitry underlying the antinociceptive action of opiates. In: Fields HL, Besson J-M, eds. *Progress Brain Research* 77. Amsterdam: Elsevier, 1988:245-257.
64. Gamble GD, Milne RJ. Hypercapnia depresses nociception: Endogenous opioids implicated. *Brain Res* 1990; 514:198-204.
65. Taveira Da Silva AM, Dias Souza J, Quest JA, et al. Central nervous system site of action for the respiratory depressant effect of diacetylmorphine (heroin) in the cat. *J Clin Invest* 1983; 72:1209-1217.
66. Dehkordi O, Dennis GC, Millis RM, et al. Effects of physostigmine on cocaine-induced cardiorespiratory responses at the caudal ventrolateral medullary surface (this volume).
67. Chiang C, Aston-Jones G. Response of locus coeruleus neurons to footshock stimulation is mediated by neurons in the rostral ventral medulla. *Neuroscience* 1993; 53:705-715.
68. Yates BJ, Bolton PS, Goto T, et al. The role of the ventral brainstem in vestibulo-sympathetic and respiratory reflexes (this volume).
69. Jennings DB, Walker JKL, Ohtake PJ. Central effects and interactions of the renin-angiotensin system and vasopressin on ventilation and PaCO₂ (this volume).
70. Spyer KM. Central nervous mechanisms contributing to cardiovascular control. *J Physiol (Lond)* 1994; 474:1-20.
71. Speck DF, Beck ER. Respiratory rhythmicity after extensive lesions of the dorsal and ventral respiratory groups in the decerebrate cat. *Brain Res* 1989; 482:387-392.
72. St John WM, Glasser RL, King RA. Rhythmic respiration in awake vagotomized cats with chronic pneumotaxic center lesions. *Respir Physiol* 1972; 15:233-244.
73. Blair RW. Convergence of sympathetic, vagal, and other sensory inputs onto neurons in feline ventrolateral medulla. *Am J Physiol (Heart Circ Physiol)* 1991; 260:H1918-H1928.
74. Koepchen HP. Respiratory and cardiovascular "centres": Functional entirety or separate structures? In: Schlaefke ME, Koepchen HP, See WR, eds. *Central Neuron Environment and the Control System of Breathing and Circulation*. Berlin: Springer-Verlag, 1983:221-237.
75. Nattie EE, Li A. Retrotrapezoid nucleus glutamate injections: Long-term stimulation of phrenic activity. *J Appl Physiol* 1994; 76:760-772.
76. Nagy F, Bal T, Cardi P. Dynamic re-wiring of CPG circuits in a simple nervous system. In: Eeckman FH, ed. *Analysis and Modeling of Neural Systems*. Boston: Kluwer, 1992:339-351.
77. Horner RL, Kozar LF, Phillipson EA. Tonic respiratory drive in the absence of rhythm generation in the conscious dog. *J Appl Physiol* 1994; 76:671-680.
78. Sears TA, Berger AJ, Phillipson EA. Reciprocal tonic activation of inspiratory and expiratory motoneurons by chemical drive. *Nature* 1982; 299:728-730.

16

Effect of CMA and MPA, Synthetic Progesterones, on Control of Respiration in Humans

YOSHIYUKI HONDA, TSUGUO MORIKAWA, HIROSHI KIMURA,
and KOICHIRO TATSUMI

Chiba University School of Medicine
Chiba, Japan

I. Introduction

Loeschcke and his associates were the first to have experimentally demonstrated augmented ventilation by progesterone administration in male and postmenopausal female subjects (1,2). They further tried to correlate this finding with central respiratory chemosensitivity by perfusing the ventrolateral surface of the medulla with progesterone-containing solution (3). The PaCO₂ ventilation (tidal volume) response curve was shown to shift to the left and the slope to increase. The possibility of the involvement of peripheral chemosensitivity was also examined, but the cross-circulation technique used by Mei et al. produced negative results (4). However, Hannhart et al. (5,6) demonstrated in pregnant cats that the carotid sinus nerve (CSN) discharge response to progressive hypoxia was enhanced, suggesting a directly stimulating influence of progesterone plus estrogen on the carotid body. However, this does not necessarily mean the presence of augmented peripheral chemoreceptor activity under natural conditions, because ventilation substantially increases and arterial blood should be hyperoxemic rather than hypoxemic in pregnancy (7).

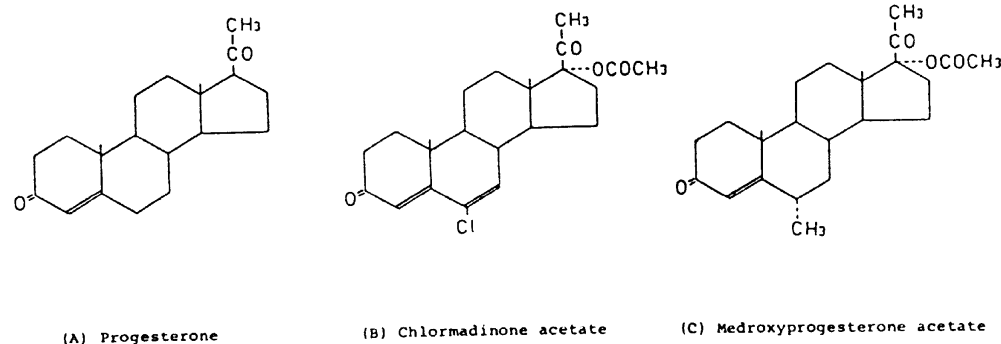


Figure 1 The chemical structures of progesterone and the synthetic progesterones used in the present study.

II. Synthetic Progesterone

In our study, we used mainly a synthetic progesterone, chlormadinone acetate (CMA), which has 10 times the progestational activity of medroxyprogesterone acetate (MPA) (8). MPA is an agent that has often been used in North America for respiratory studies and treatment. For comparison with CMA, MPA was also tested in our study. Since MPA is 15 times more active than natural progesterone (9), CMA is considered to be as much as 150 times stronger than natural progesterone. The presence of chlorine in the compound induces potentiation of luteinizing activity. Figure 1 compares the chemical structures of progesterone, CMA, and MPA.

III. Effect of Synthetic Progesterones on Respiratory Activities

A. Outline of Study Methods

First, 16 normal male subjects (25 ± 2.7 years of age) were administered CMA, MPA, and placebo in a randomized double-blind crossover maneuver (10). CMA and MPA were administered orally at a dose of 25 mg twice a day for 7 days. The placebo tablet, identical in appearance to the test drugs, contained lactose and was also given twice a day for 7 days. To make sure that the drug effect had sufficiently worn off, an interval of more than 2 weeks was allowed between each drug administration run. Just before and again on the last day of drug administration, the subjects were examined between 9 and 10 A.M. for the following: body weight, oral temperature, heart rate, venous blood sampling to measure various hormones and neuropeptides, arterial blood drawn to measure blood gas and acid-base balance, pulmonary function, ventilatory

pattern, metabolic rate measured by $\dot{V}O_2$ and $\dot{V}CO_2$, and finally hypercapnic and hypoxic ventilatory responses (HCVR and HVR) by Read's rebreathing method and the progressive isocapnic hypoxia test respectively. To evaluate the magnitude of the ventilatory drive, both the amount of minute ventilation and height of occlusion pressure were measured. For the latter item, we used $P_{0.2}$ which was the occluded inspiratory airway pressure obtained at 0.2 s after the onset of inspiration; this was found to be more reproducible than the conventionally used $P_{0.1}$ (11). Furthermore, a number of patients with prostatic hypertrophy (12), chronic obstructive pulmonary disease (COPD) (13–15), and

Table 1 Body Weight, Body Temperature, Heart Rate, Pulmonary Function, Arterial Blood Gases, Alveolar Ventilation and Metabolic Rate with Placebo, CMA, and MPA Treatments ($n = 16$)^a

	Placebo	CMA	MPA
Body weight, kg	67.7 ± 1.4	67.4 ± 1.5	67.4 ± 1.4
Body temp, °C	36.5 ± 0.1	36.8 ± 0.1 ^b	36.7 ± 0.1
Heart rate, beats/min	70.1 ± 1.9	67.9 ± 1.4	68.3 ± 1.5
Pulmonary function			
%VC	104.7 ± 3.2	103.6 ± 2.8	101.6 ± 3.5
FEV _{1.0%}	86.1 ± 1.6	86.3 ± 1.4	85.9 ± 1.3
Arterial blood			
pH	7.39 ± 0.01	7.40 ± 0.06	7.40 ± 0.01
PaCO ₂ , mm Hg	39.4 ± 0.7	35.4 ± 0.7 ^c	36.5 ± 0.8 ^c
PaO ₂ , mm Hg	91.9 ± 1.4	95.4 ± 1.2	94.4 ± 1.5
[HCO ₃ ⁻], mM/L	23.1 ± 0.3	21.0 ± 0.3 ^c	21.8 ± 0.4 ^c
Ventilation			
\dot{V}_A , L/min	4.36 ± 0.20	5.40 ± 0.30 ^c	5.07 ± 0.25 ^c
V _T , liters	0.59 ± 0.03	0.63 ± 0.04	0.63 ± 0.04
f, breaths/min	15.8 ± 1.4	17.1 ± 1.7	17.3 ± 1.6
V _T /T _I , L/s	0.41 ± 0.02	0.43 ± 0.02	0.44 ± 0.02
P _{0.2} , cm H ₂ O	3.7 ± 0.2	3.8 ± 0.3	4.3 ± 0.3
V _D /V _T	0.32 ± 0.02	0.28 ± 0.03	0.30 ± 0.02
Metabolic rate			
$\dot{V}CO_2$, mL/min	194 ± 7	218 ± 10	213 ± 10
$\dot{V}O_2$, mL/min	247 ± 11	273 ± 14	274 ± 12

^aValues are mean ± SE. CMA, chlormadinone acetate; MPA, medroxyprogesterone acetate; %VC, vital capacity of the predicted value in %; FEV_{1.0%}, forced expiratory volume in 1 s in percent for forced vital capacity; \dot{V}_A , minute alveolar ventilation; V_T, tidal volume; f, breathing frequency; T_I, inspiratory duration; P_{0.2}, mouth occlusion pressure at 0.2 s after onset of inspiratory effort; V_D/V_T, ratio of dead space to tidal volume.

^bSignificant difference between placebo and MPA or CMA data, $P < 0.05$.

^cSignificant difference between placebo and MPA or CMA data, $P < 0.01$.

From reference 9: reproduced by permission.

sleep apnea syndrome (SAS) (16) were treated with CMA; a beneficial effect was seen in a substantial number of cases. The underlying pathophysiological mechanisms for this improvement were also pursued.

B. Ventilatory Pattern and Ventilatory Responses

Table 1 represents the physical condition, pulmonary function data, blood gas, and metabolic rate at rest after drug administration. Compared with the placebo run, the acid-base status of the arterial blood clearly indicates the presence of respiratory alkalosis by CMA and MPA ingestion, and this was derived from increases in both \dot{V}_T and f , resulting in significant augmentation in \dot{V}_A . On the other hand, no definite changes were detected in body weight, heart rate, pulmonary function, or metabolic rate.

P_{ETCO_2} ventilation response curves shifted to the left and their slopes tended to increase with synthetic progesterones (Fig. 2). When the subjects were loaded with inspiratory flow resistance in an amount of 16 cm H₂O/L/s at a flow rate of 1.0 L/s, the drug effect was better demonstrated. Furthermore, the response curves evaluated in terms of occlusion pressure were found to better represent the augmented response by CMA and MPA (Fig. 3).

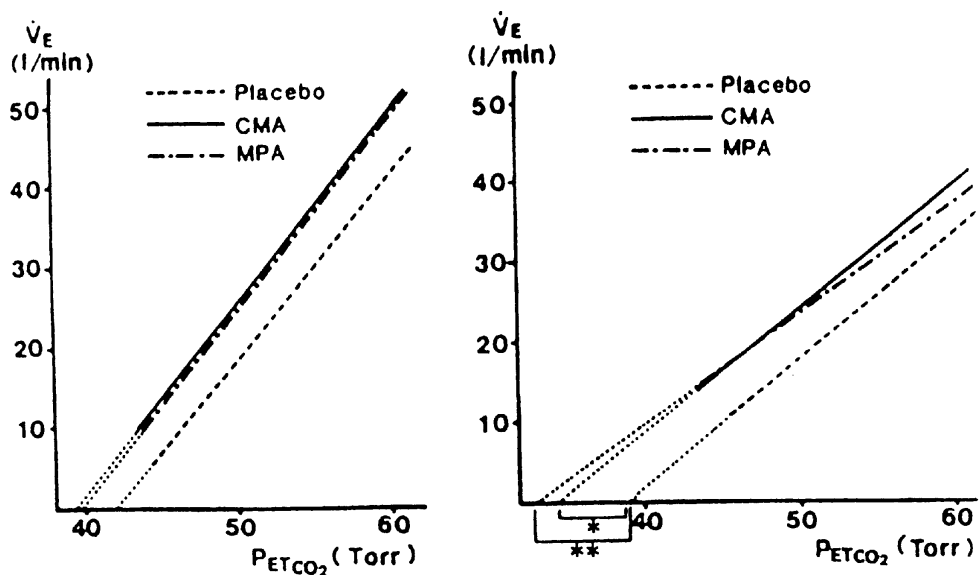


Figure 2 Mean ventilatory response (\dot{V}_E) to CO₂ in unloaded (left) and loaded (right) conditions. * $0.05 < P < 0.01$, ** $P < 0.05$: differences in horizontal intercept of \dot{V}_E end-tidal PCO₂ (P_{ETCO_2}) response line between placebo and chlormadinone acetate (CMA) or medroxyprogesterone acetate (MPA) data are of borderline significances at a 10% level and significant at a 5% level, respectively. (From Ref. 9.)

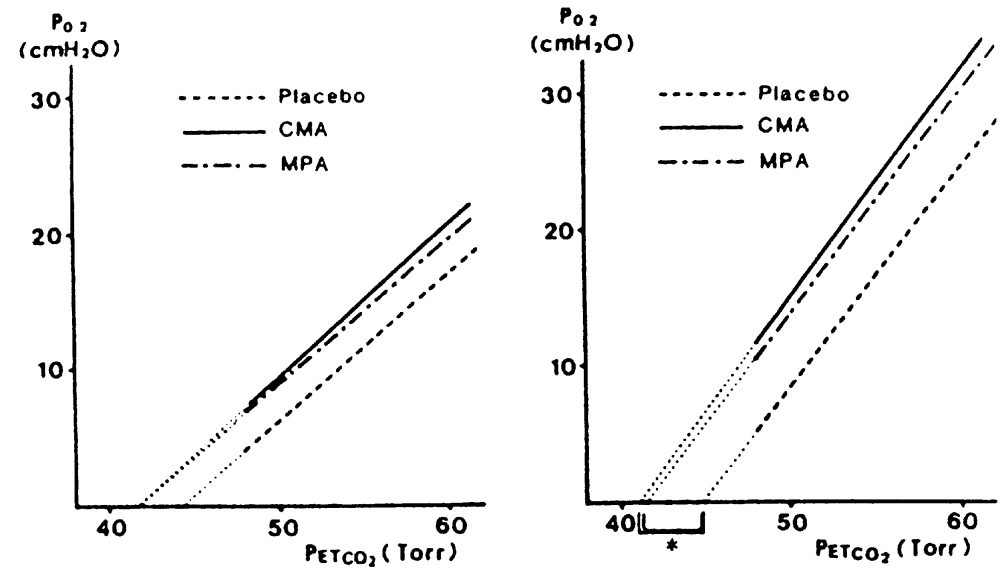


Figure 3 Mean occlusion pressure response to CO₂ in unloaded (left) and loaded (right) conditions. * $0.05 < P < 0.1$: difference in horizontal intercept of occlusion pressure at 0.2 s after inspiratory effort end-tidal PCO₂ ($P_{O_2} - P_{ETCO_2}$) response line between placebo and chlormadinone acetate (CMA) or medroxyprogesterone acetate (MPA) data are of borderline significance at a 10% level. (From Ref. 9.)

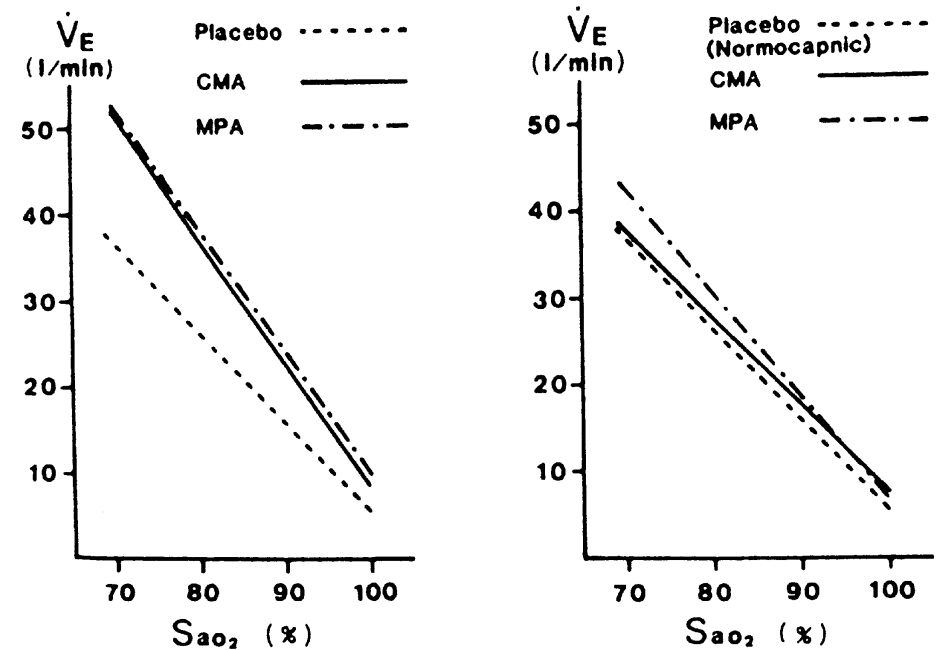


Figure 4 Mean ventilatory response (\dot{V}_E) to hypoxia in normocapnic (left) and hypocapnic (right) conditions. Dashed line representing placebo data is the normocapnic response curve because PaCO₂ was not decreased in this condition. CMA, chlormadinone acetate; MPA, medroxyprogesterone acetate; SaO₂, arterial O₂ saturation. (From Ref. 9.)

SaO₂ ventilation and occlusion pressure response curves exhibited a shift to the right and increased slope (Figs. 4 and 5). This tendency was pronounced when tested under normocapnic conditions and was distinct when evaluated by the occlusion pressure.

C. Load Compensation Response

Figure 6 illustrates the P_{ET}CO₂ ventilation response curves before and after CMA in 10 patients with prostatic hypertrophy without cardiorespiratory complication. Augmented ventilatory drive response to flow-resistive loading (i.e., increased occlusion pressure response) is the most pronounced feature demonstrated in this figure. The degree of increased occlusion pressure in response to flow-resistive loading in 12 COPD patients was plotted on the ordinate axis and termed the load compensation ratio (LCR) (Fig. 7). The magnitude of LCR is known to be correlated with higher central nervous system (CNS) activity

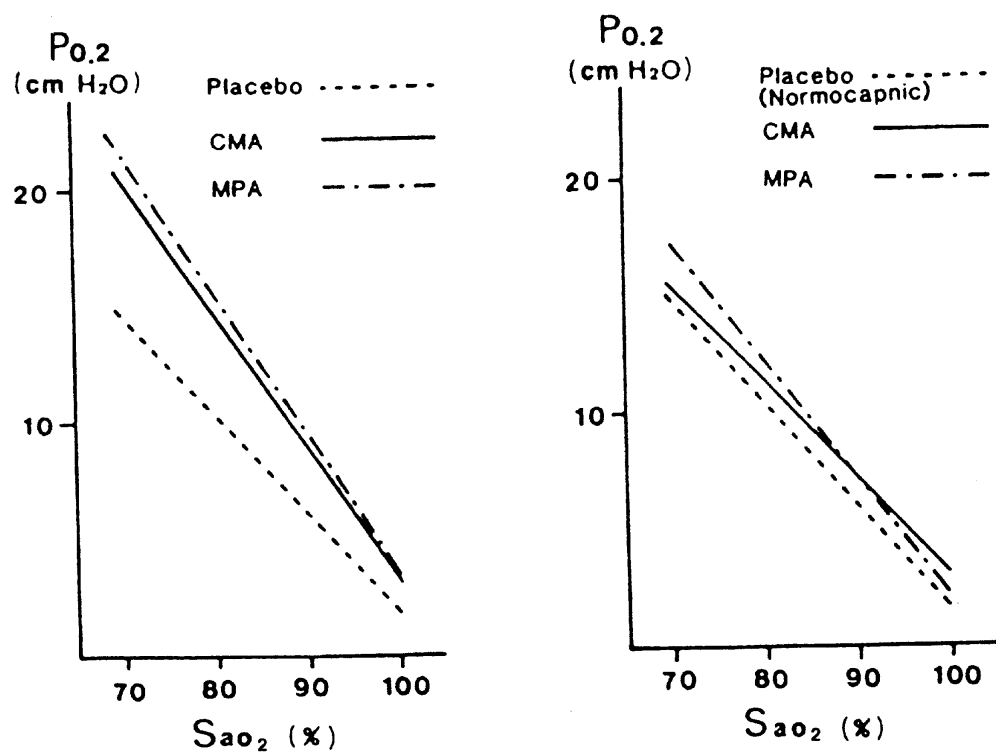


Figure 5 Mean occlusion pressure response ($P_{0.2}$) to hypoxia in normocapnic (left) and hypocapnic (right) conditions. Placebo responses indicated by dashed lines in both figures are normocapnic, as explained in Figure 4. (From Ref. 9.)

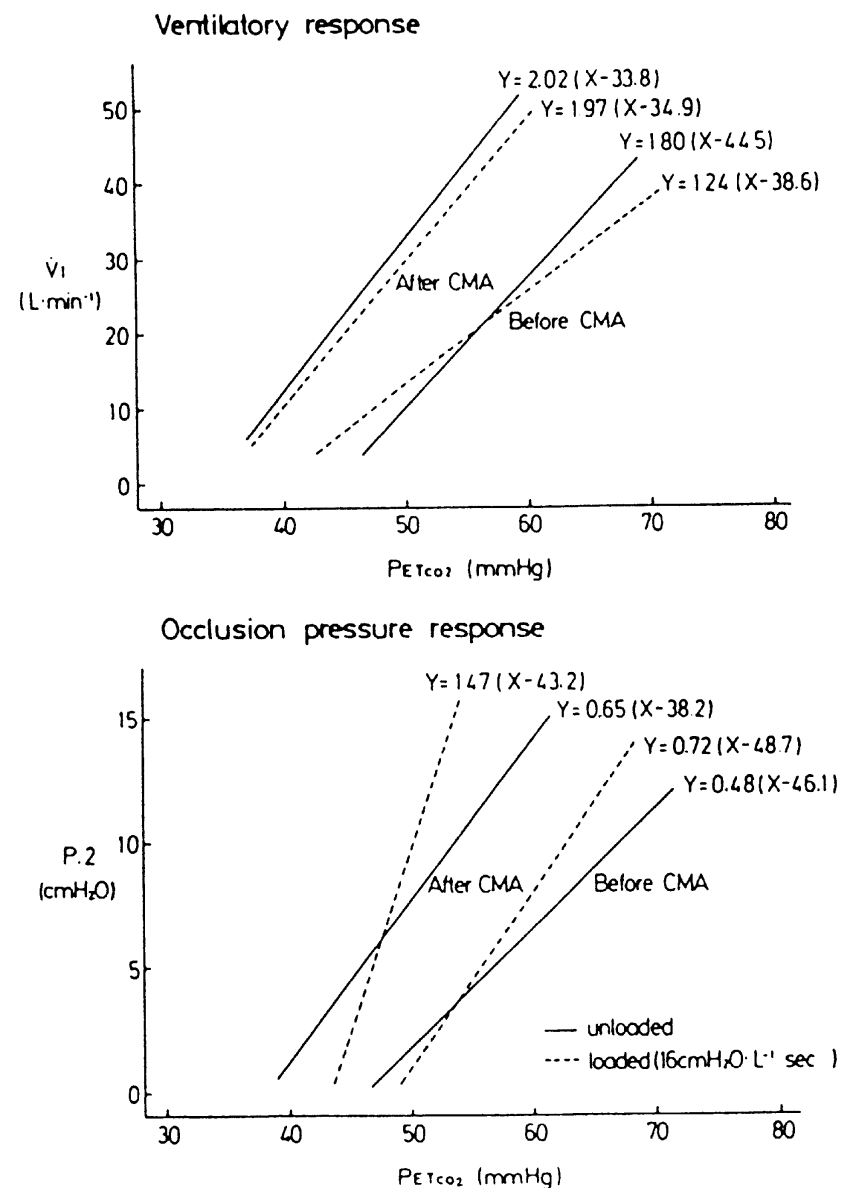


Figure 6 Mean ventilatory and occlusion pressure response lines to CO₂. Solid line, response line without loading; dashed line, response line with loading; \dot{V}_t , inspired minute ventilation; CMA, chlormadinone acetate; P_{ET}CO₂, end-tidal PCO₂; P_{0.2}, occlusion pressure at 0.2 s. (From Ref. 11.)

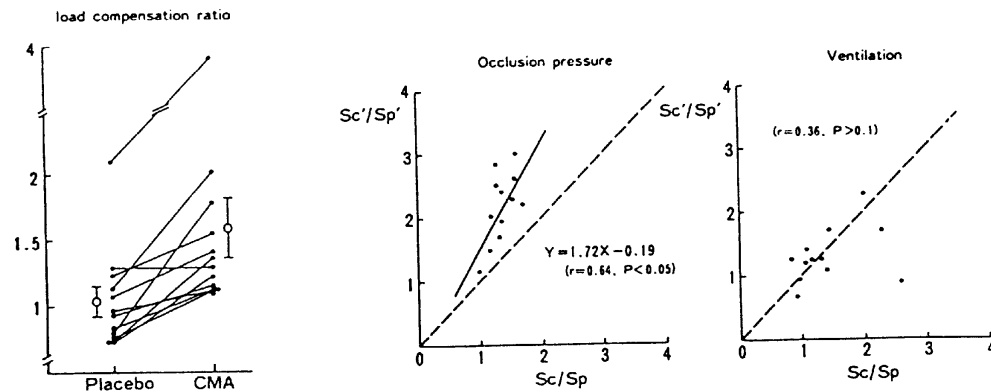


Figure 7 Left panel: Changes of inspiratory flow-resistive load compensation with placebo and CMA therapy. The change of load compensation is expressed as the ratio of loaded to unloaded $\Delta P_{0.2}/\Delta P_{CO_2}$. Closed circles and solid lines indicate individual data; open circle with vertical bar represents mean \pm SE. Middle and right panels: Relationship between chemical and neuromechanical drives with placebo against CMA conditions. Subscripts p and c indicate placebo and CMA, respectively; prime indicates the condition with flow-resistive loading; Sp and Sp' are the slopes of ventilatory and occlusion pressure responses in unloaded and loaded condition, respectively, with placebo treatment; Sc and Sc' are the same as above with CMA therapy. The middle panel shows the relationship of occlusion pressure response to CO_2 , and the right panel that of ventilatory response to CO_2 . (From Ref. 12.)

and is effectively and disproportionately augmented by CMA, as shown in the middle section of this figure. Since occlusion pressure independently assesses the ventilatory drive regardless of alterations in mechanical properties of the airways, we consider LCR to be a good indicator for evaluating the ventilatory effect of CMA. In 9 SAS patients, parallel increases in both hypercapnic ventilation and occlusion pressure responses were observed in 7 out of 9 subjects (Fig. 8), and this was found to be a useful indication of improvement in clinical symptoms (16).

IV. Hormones and Neuropeptides After Administration of Synthetic Progesterone

Table 2 shows the level of certain hormones and neuropeptides after placebo, CMA, and MPA administration. Both TSH and ACTH showed a tendency to be increased by synthetic progesterones, and particularly for augmentation of TSH was shown to be a significant level by MPA. This is in contrast to the levels of T_3 and T_4 as shown in Figure 9. Figure 10 illustrates a possible mechanism

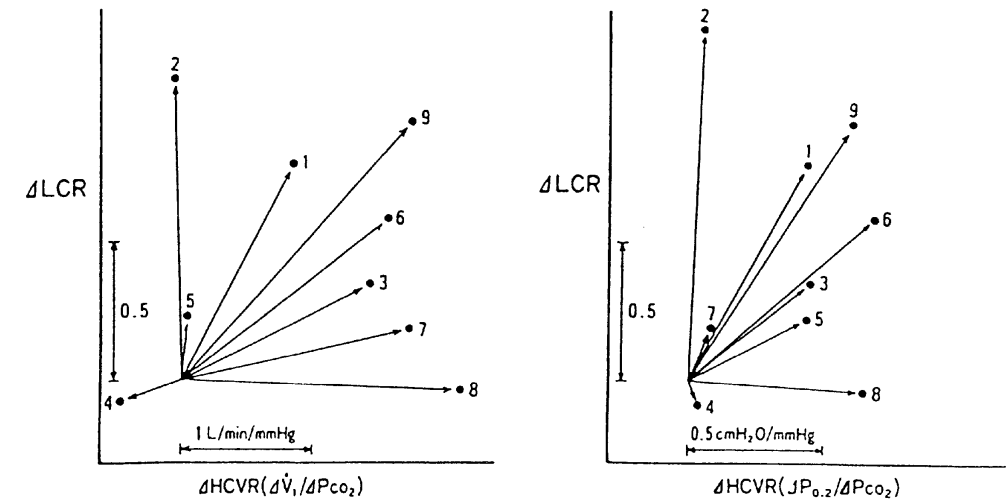


Figure 8 Relationship between the amount of change in load compensation ratio (ΔLCR) and that in hypercapnic ventilatory response ($\Delta HCVR$) demonstrated by a vector. $\Delta HCVR$ in the left and right panels shows the change in hypercapnic ventilatory and occlusion pressure responses, respectively. Numbers are patient numbers. (From Ref. 15.)

Table 2 Effect of Placebo, CMA and MPA Administration on Certain Hormones and Neuropeptides

		Placebo (n = 13)	CMA (n = 12)	MPA (n = 13)
TSH	(μ U/ml)	1.98 \pm 0.21	2.45 \pm 0.36	2.72 \pm 0.32*
T_3	(ng/ml)	156.9 \pm 8.4	156.2 \pm 4.5	164.2 \pm 8.0
T_4	(μ g/ml)	9.31 \pm 0.43	9.18 \pm 0.32	10.12 \pm 0.44
ACTH	(pg/ml)	4.70 \pm 3.24	8.65 \pm 4.71	6.75 \pm 3.53
Cortisol	(ng/ml)	160.4 \pm 19.8	141.7 \pm 19.0	174.7 \pm 19.9
Adrenaline	(ng/ml)	0.040 \pm 0.013	0.032 \pm 0.007	0.035 \pm 0.008
Noradrenaline	(ng/ml)	0.25 \pm 0.03	0.25 \pm 0.02	0.26 \pm 0.03
Dopamine	(ng/ml)	<0.2	<0.2	<0.2
Serotonin	(ng/ml)	76.9 \pm 9.1	75.5 \pm 8.7	81.5 \pm 9.8
β -endorphin	(pg/ml)	17.3 \pm 3.1	17.1 \pm 2.4	20.3 \pm 2.5

Values are mean \pm SE.

* $P < 0.05$: difference between placebo and MPA data is significant at 5% level.